KA-TO-L-BAND FREQUENCY DOWN-CONVERSION USING A MICRO-PHOTONIC III-V-ON-SILICON MODE-LOCKED LASER AND MACH-ZEHNDER MODULATOR

K. Van Gasse[1,2*], Z. Wang[1,2**], S. Uvin[1,2], B. De Deckere[3], J. Mariën[3], L. Thomassen[3], G. Roelkens[1,2]

[1]*Photonics Research Group, INTEC-department, Ghent University-IMEC, Belgium.*
[2]*Center for Nano- and Biophotonics, Ghent University, Belgium*
[3]*Antwerp Space, Berkenrodelei 33, 2260 Hoboken, Belgium*
*kasper.vangasse@ugent.be, **zhechao.wang@intec.ugent.be

I. INTRODUCTION

RF frequency down-conversion is of key importance in communication satellites. While the available high-end microwave electronic mixers and circuitry are bulky, heavy, expensive and sensitive to electromagnetic interference (EMI), microwave photonics emerges to be a promising and low-cost alternative. In this case, the local oscillator RF signals can be distributed using optical fiber instead of electrical connections, bringing important advantages in terms of mass, power and volume. Ultra-compact photonic frequency down-converters can be realized by the means of photonic integration, which again greatly reduces the footprint and weight of the microwave system compared to legacy solutions. Over the past decade, the III-V-on-Silicon hybrid integration platform has been developed into a relatively mature technology that enables applications in various fields. It combines passive silicon-on-insulator (SOI) photonic integrated circuits (PIC), with III-V semiconductor based active devices such as high-speed modulators, photodiodes and lasers. Such a platform allows creating a compact Electro-Photonic Frequency Converter (EPFC) consisting of integrated photonic components.

II. ELECTRO-PHOTONIC FREQUENCY CONVERTER CONCEPT

The architecture of the EPFC is shown in Fig. 1(a) and is based on three key integrated photonic components: a mode-locked laser (MLL), a dual-drive Mach-Zehnder Modulator (DDMZM) and a photodiode. The MLL generates an optical pulse train which is then modulated by the DDMZM. The RF signal (in the Ka-band) serves as an input for the DDMZM, and the optical pulses subsample the RF signal generating the desired IF signal. A photodiode collects the modulated pulses such that its output contains a down-converted version of the Ka-band channel.

The operation principle for the down-conversion of a 500 MHz channel with a carrier frequency of 29.25 GHz is shown in Fig 1(b). The repetition rate of the MLL is designed to be 15.95 GHz, which allows achieving a 500 MHz channel free of spurious peaks generated by other harmonic frequency mixing components. The DDMZM consists of a Mach-Zehnder interferometer structure, in which both arms contain a high-speed optical phase shifter that can be driven independently. The top arm is driven by the RF input while the bottom arm is driven by a LO, which is used to select a channel in the Ka-band to be down-converted to the IF. When the optical pulses are modulated with a sine of 29.25 GHz the optical carrier frequencies will have sidebands spaced 29.25 GHz from the carrier (see (1) and (2)). The bottom arm optical phase shifter modulates the optical pulses with a 4.15 GHz LO tone (see (3)). By combining the modulated pulses from both arms, the RF and LO sidebands are spaced by the targeted IF frequency (see (4)). Furthermore, the top and bottom arm are biased in such a way that they have a π phase difference, which cancels out the optical carriers. This avoids saturation of the photodetector by the intense optical pulses from the mode-locked laser. The photodiode output is generated by the beating of the different optical sidebands. The frequency of the different beatings correspond to the mixing of the repetition frequency of the modelocked laser, the RF modulation frequency and the LO modulation frequency. It can be summarized with the formula

$$f_{signal} = m \cdot f_{rep} \pm f_{RF} \pm f_{LO} \tag{1}$$

The IF signal is generated by the beating of $2 \cdot f_{rep} - f_{RF} - f_{LO}$. Because the output of the photodiode will contain all possible beating terms at different frequencies, a bandpass filter is needed after the photodiode to extract the correct IF output.
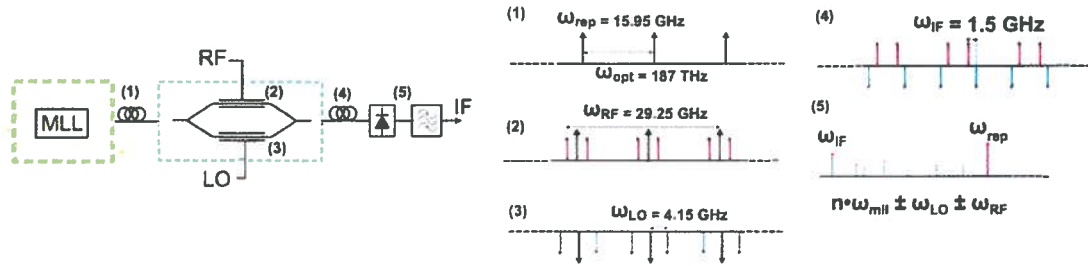
Figure 1: (a) Schematic representation of the EPFC architecture; (b) corresponding optical spectra / RF spectra at various points in the system: (1) MLL output (2) RF modulation of MLL output (3) LO modulation of MLL output (4) Optical output of the MZM (5) Electrical output of the photodiode, containing the IF signal and several spurious peaks. The frequency of the peaks is given by combinations of the rep rate, RF frequency and LO frequency.

Apart from the frequency scheme, the power efficiency of the EPFC is of paramount importance. The transfer function, being the ratio of the IF output power to the RF input signal power, can be found to be [1]

$$G = \mathcal{R}^2 P_{in}^2 G_{Ext}^2 t_{ff}^2 J_1(\beta_{LO})^2 \left(\frac{\pi}{V_\pi}\right)^2 R_{in} R_{out} \qquad (2)$$

where $\mathcal{R}$ is the photodiode responsivity, P_{in} is the average optical output power generated by the MLL, G_{Ext} is the external optical gain and t_{ff} represents the optical insertion loss of the modulator and fiber-chip coupling. The term $J_1(\beta_{LO})$ represents the modulation efficiency, where $\beta_{LO} = \pi V_{LO}/V_\pi$ is the modulation index. Finally R_{in} is the input impedance of the modulator and R_{out} is the load resistance coupled to the photodiode. From this formula it is clear that both the efficiency of the modulator (i.e. the V_π) and the optical loss are important factors that affect performance of the EPFC.

III. MODE-LOCKED LASER

The short pulse train is generated by a III-V-on-Silicon MLL operating at 1570 nm, which is realized by the adhesive bonding of a III-V die on a SOI PIC containing waveguides, gratings and other passive structures. The III-V active photonic components are afterwards defined by contact lithography, wet/dry etching and metallization. A more detailed description of the process can be found in [2]. A schematic design of the MLL can be found in Fig. 2. A so-called anti-colliding pulse configuration is adopted to achieve high optical output power and short optical pulses [3]. The laser cavity is formed by a low and a high reflectivity grating etched into the silicon waveguide. An InP-based optical amplifier is formed on top of the silicon waveguide, and optical coupling is achieved by tapering both Si and InP waveguides. On top of the low-reflective grating, a part of the InP waveguide is electrically isolated to form a saturable absorber (SA), thereby dividing the gain section in two parts. Finally the laser cavity also contains a long spiral silicon waveguide, the length of which is designed to target the required repetition rate of the MLL. In Fig. 2(c) a microscope image shows the MLL is electrically contacted using a custom RF probe.
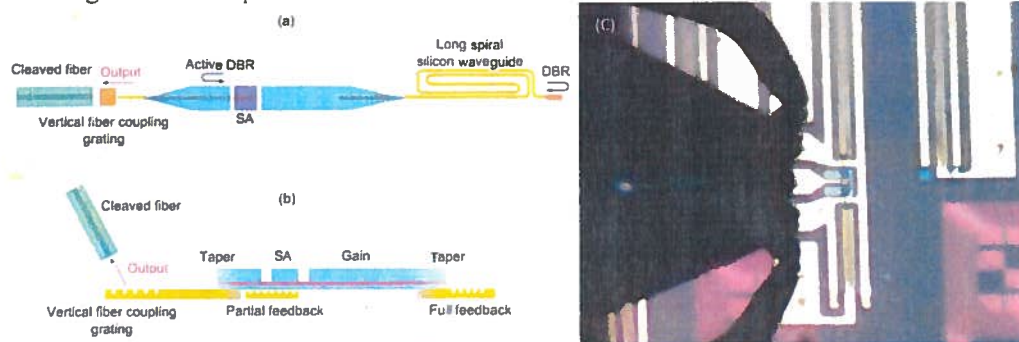

Figure 2: (a) Schematic top view of the III-V-on-Silicon MLL (b) Schematic side view of the III-V-on-Silicon MLL (c) Microscope image of the PIC contacted using an RF probe.

IV. MACH-ZEHNDER MODULATOR

The Mach-Zehnder modulator was realized on the III-V-on-Silicon platform as well. Another InP wafer with a different epitaxial layer design was used for the modulator. The achieved bandgap offset allows for efficient phase modulation of the optical pulses generated by the MLL. A microscope image of the modulator is shown in

figure 3. The Mach-Zehnder structure is created by low-loss optical silicon waveguides, which are 400 nm thick and 650 nm wide. The Mach-Zehnder interferometer further contains two 2 by 2 multi-mode interferometer 3dB splitters (MMIs), such that the output can be directed to an on-chip photodiode or a vertical fiber grating coupler. A taper structure similar to the laser design is used to couple the light from the silicon waveguide to the InP phase shifting section and vice versa. The phase shift section is 1.5 mm long and is driven by a travelling wave electrode. The segmented design enables a group velocity matching between the optical pulse propagating in the Si waveguide and the electrical wave propagating through the travelling wave electrodes. This matching increases the bandwidth of the modulator. Both the RF and LO signals are delivered to the modulator by 100 micron pitch gold bond pads. In our experiments the modulators were contacted with RF probes, although the chips can also be co-integrated with electronic driver circuits using wire bonding. Furthermore, bond pads for external termination of the travelling wave electrode are provided. A thermo-optic phase shifter in the bottom arm allows biasing the modulator for optical carrier cancellation as discussed above.
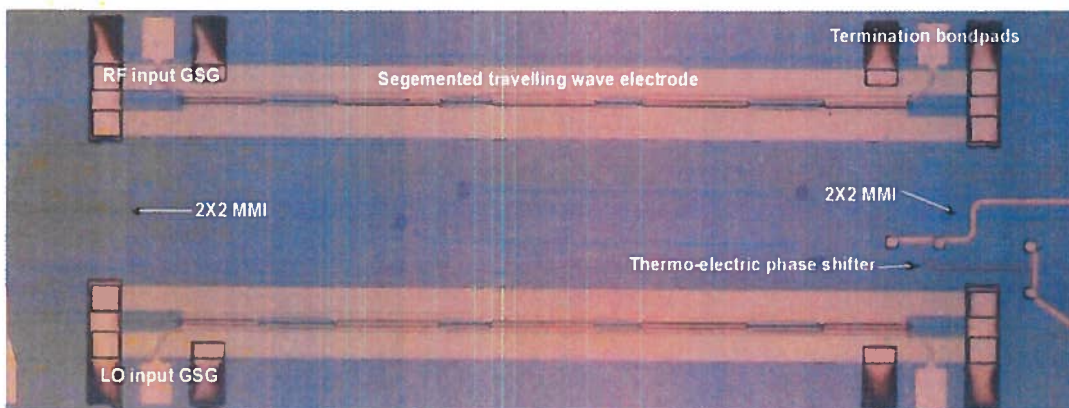

Figure 3: Microscope image of the III-V-on-Silicon Mach-Zehnder Modulator.
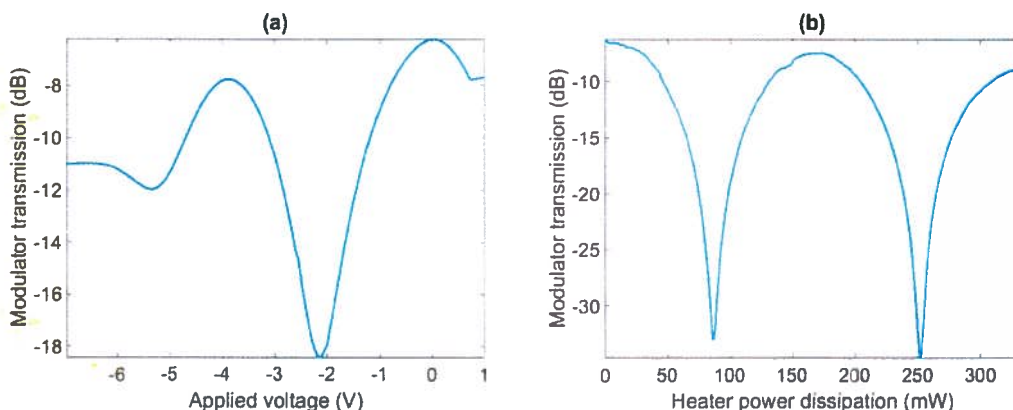

Figure 4: (a) Modulator transmission as a function of the voltage applied to the InP phase shifter. (b) Modulator transmission as a function of the power dissipated in the thermo-optic phase-shifter.

Fig. 4(a) shows the transmission of the modulator as a function of the voltage applied to the top phase shifter of the MZM. The modulator shows a Vpi of 2 V and an insertion loss of 6 dB, not including the loss of the fiber-to-chip grating couplers. The extinction ratio drops as the voltage increases, as the increased absorption loss in only one arm unbalances the optical power between the two arms, leading to imperfect destructive interference. In Fig. 4(b) the modulator transmission as a function of the electrical power supplied to the bias heater is shown. An extinction ratio of 25 dB is achieved when the high-speed phase shifters are equally biased.

V. DOWN-CONVERSION EXPERIMENT

In this section we present the down-conversion of five 500 MHz wide Ka-band channels to L-band using the afore-discussed electro-photonic frequency converter. A commercial Discovery Semiconductors photodiode with a TIA was used as receiver. A schematic of the measurement setup is shown in Fig 5. Both the MLL and MZM chips were mounted on temperature controlled chucks. RF and DC probes were used to contact the chips.
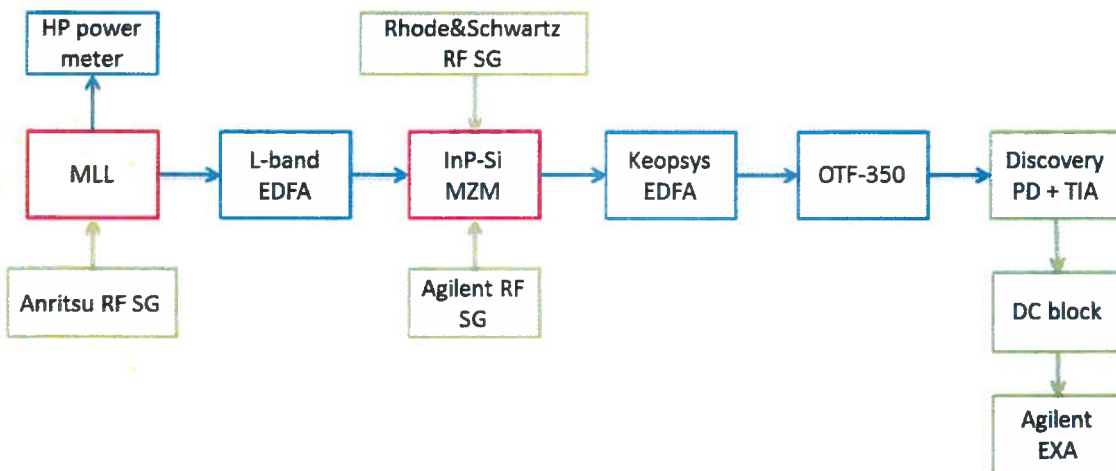
Figure 5: Overview of the measurement set-up. Electrical connections and devices are in green, optical devices and connections in blue and the silicon photonic devices are in red.

In order to down-convert five Ka-band channels centered at 27.75, 28.25, 28.75, 29.25 and 29.75 GHz to the same IF frequency, a frequency scheme has to be devised such that for a chosen MLL rep rate and LO frequency no spurious peaks are located in a 500 MHz interval around 1.5 GHz. Therefore the rep rate of the MLL is designed to be 15.95 GHz and the LO frequency is chosen as 3.65, 4.15, 4.65, 5.15 and 5.65 GHz for the 5 Ka-band channels, respectively. The MLL had a fundamental repetition rate of 2.6 GHz and was harmonically mode-locked to 15.584 GHz using an Anritsu RF signal generator. Although the rep rate deviates from the optimal design, by slightly adjusting the LO frequency, an IF frequency of 1.5 GHz can still be achieved.

The average fiber-coupled optical output power of the MLL is −7 dBm and is centered at 1573 nm. To compensate for the fiber-chip coupling losses, the optical signal is amplified using an L-band Erbium Doped Fiber Amplifier (EDFA). The pulses are then coupled into the III-V-on-Silicon MZM chip again using a vertical grating coupler. The modulator described above is driven using a Rhode & Schwarz signal generator for RF input and an Agilent signal generator for the LO. The light collected from the output of the modulator is amplified using a Keopsys EDFA to compensate coupling losses again. A Santec optical tunable filter is used to filter out the EDFA noise. The optical signal is detected by a Discovery Semiconductors 30 GHz photodiode and 26 GHz trans-impedance amplifier. The generated RF spectrum is analyzed using a Keysight electrical spectrum analyzer. An example of the electrical spectrum is shown in Fig. 6(a). Besides the targeted 1.5 GHz IF signal, many spurious peaks also exist, which need to be filtered out. However, all measured spurious peaks matched the calculated beating frequencies and can therefore be exactly predicted.

For all 5 Ka-band channels, the RF input is scanned over a 700 MHz band range to verify the flatness of the down-converted channel and the absence of spurious peaks in the IF band. The down-conversion of the 27.75 and 28.25 GHz channel is shown in Fig 6(b). A flat response over 700 MHz independent of the channel can be found. The small variations that can be seen in conversion efficiency over the 700 MHz band are due to optical power fluctuations caused by the vertical fiber coupling scheme, which can easily be overcome in a fully packaged EPFC. It should be stressed that in this demonstration no equalization was used.

The achieved conversion efficiency in this demonstration is not representative of the final target as some experimental limitations can be overcome in a packaged and fully integrated version of this EPFC. The efficiency of the modulator was limited as it was not possible to probe both arms separately while at the same time terminating the travelling wave electrodes, limiting the efficiency of the modulator in the Ka-band. In a future iteration semiconductor optical amplifiers (SOAs) will be co-integrated on-chip to boost the optical power, eliminating the use of EDFAs. Furthermore the grating coupling losses can be optimized, which could dramatically improve the conversion efficiency. Integrating the photodiode with the MZM can eliminate the extra coupling losses and the noise from amplification as well. Implementing these changes, a conversion efficiency of -20 dB can be expected.
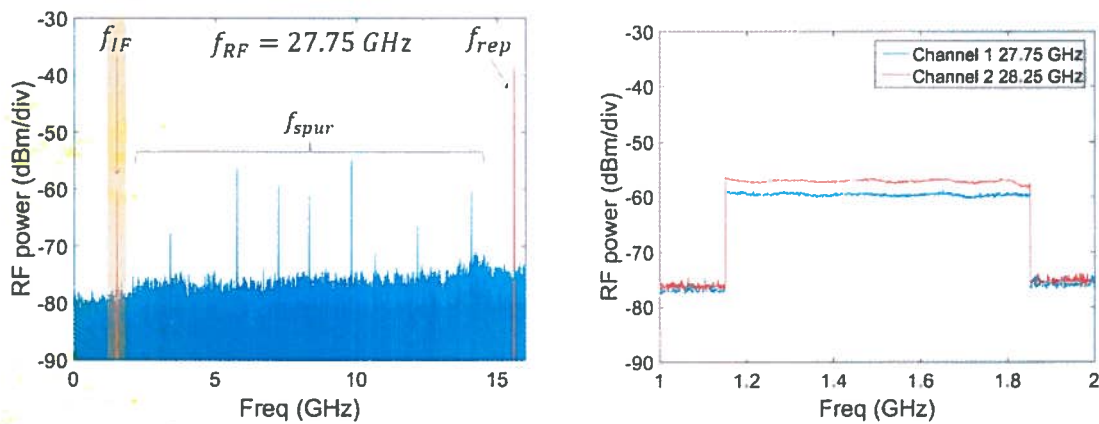
Figure 6: (left) RF spectrum created by the EPFC with the IF band highlighted as well as the strong signal corresponding to the repetition rate of the MLL. (right) Resulting IF of two down-converted channels where the input frequency is swept over a 700 MHz band. This shows the flat response of the channel as well as the absence of spurious peaks.

VI. CONCLUSION

We have demonstrated an Electro-Photonic Frequency Converter (EPFC) based on integrated photonic components. Both the mode-locked laser and Mach-Zehnder modulator were realized on the III-V-on-Silicon platform. The performance of the devices can rival existing table top microwave photonic devices in terms of bandwidth and efficiency, while reducing size and weight by orders of magnitude. The scheme provides great flexibility as input and output frequency can be changed by adjusting the repetition rate of the mode-locked laser or simply tuning the low-frequency LO.

REFERENCES

[1] E. H. W. Chan and R. A. Minasian, "Microwave Photonic Downconverter With High Conversion Efficiency," in Journal of Lightwave Technology, vol. 30, no. 23, pp. 3580-3585, Dec.1, 2012.
[2] G. Roelkens et al, "III-V-on-silicon photonic devices for optical communication and sensing," Photonics, 2(3), p.969-1004, 2015
[3] J. Javaloyes, S. Balle, "Anticolliding design for monolithic passively mode-locked semiconductor lasers," Optics letters, vol. 36, nr. 22, pp. 4407-4409, Nov. 2011.